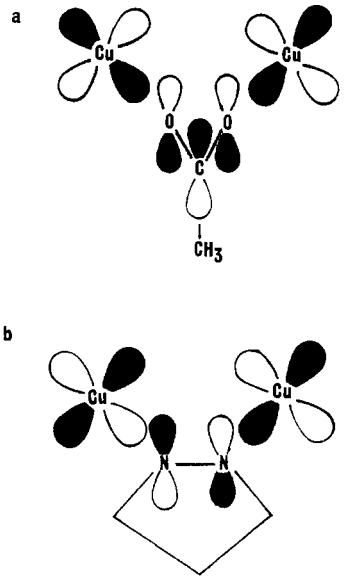

Figure 7. Orbital complementarity for binding of bridging (a) acetate and (b) pyrazolate between the Cu atoms.

described by Reed, the polarities of the $d_{x^2-y^2}$ orbitals in the present compounds are not restricted by the bridging phenoxide oxygen atom. The presence of only a single ligand mediating the magnetic interaction between the Cu atoms results in the relatively weak antiferromagnetism of complexes **9** and **10**. It appears that a bridging pyrazolate group is capable of effecting a stronger antiferromagnetic interaction between the participant metals than a bridging acetate group.

Summary. The system described and characterized herein provides some important features for an effective Hc model. The metal coordination spheres, Cu-Cu separations, spectroscopic properties, and reactivity with small-molecule substrates indicate that **5** is a reasonable model for the binuclear Cu site of EPR-detectable forms of met-Hc. Magnetic properties of the derivatives of **5**, in which exogenous ligands have been incorporated, do not mimic the protein derivatives. It is apparent that these complexes do not adopt an orientation in which a strong superexchange interaction between the Cu atoms occurs. Modifications of this system designed to encourage such interactions are the subject of current interest.

Acknowledgment. The NSERC of Canada is thanked for financial support of this research. Dr. P. E. Doan, Dr. A. Ozarowski (University of Windsor), and Dr. P. K. Mascharak (University of California, Santa Cruz) are thanked for assistance in recording EPR spectra. Dr. A. Ozarowski and Dr. P. E. Doan are also thanked for programming assistance. Dr. R. Frankel is thanked for assistance in the operation of the susceptometer at the National Magnet Laboratory. H.P.B. is grateful for the awards of Ontario Graduate and NSERC postgraduate scholarships.

Supplementary Material Available: Electrochemical data (Table S1) and magnetic susceptibility data (Tables S2-S5) (9 pages). Ordering information is given on any current masthead page.

Contribution from the Department of Chemistry, Thimann Laboratories, University of California, Santa Cruz, California 95064, and Department of Chemistry and Biochemistry, University of Windsor, Windsor, Ontario, Canada N9B 3P4

Synthetic Analogue Approach to Metallobleomycins. 2. Synthesis, Structure, and Properties of the Low-Spin Iron(III) Complex of *N*-(2-(4-Imidazolyl)ethyl)pyridine-2-carboxamide

Xiaolin Tao,[†] Douglas W. Stephan,[‡] and Pradip K. Mascharak*[†]

Received October 2, 1986

Reaction of the peptide ligand PypepH (**1**), which resembles part of the metal-chelating section of bleomycins (BLM), with $(Et_4N)[FeCl_4]$ in ethanol affords the iron(III) complex $[Fe(Pypep)_2]Cl\cdot 2H_2O$ (**2**). The structure of this synthetic analogue of Fe(III)-BLM is reported. The complex crystallizes in the triclinic space group $P\bar{1}$ with a = 11.080 (5) Å, b = 9.319 (4) Å, c = 13.665 (5) Å, α = 112.75 (3)°, β = 103.92 (3)°, γ = 73.53 (3)°, and Z = 2. The structure was refined to R = 4.46% by using 1938 unique data ($F_o^2 > 3\sigma(F_o^2)$). The coordination geometry around iron(III) is octahedral with average Fe-N(imidazole) = 1.952 (4) Å and Fe-N(pyridine) = 1.982 (4) Å, respectively. The Fe(III)-N(peptide) bond is 1.957 (4) Å long. The complex is isolated as the *mer* isomer. Variable-temperature Mössbauer spectra and magnetic susceptibility measurement at ambient temperature reveal that the iron is in the +3 oxidation state with a low-spin electronic configuration. The dark red ferric complex (**2**) can be electrochemically and chemically reduced to purple ferrous species. The electronic absorption spectrum of the reduced species is reported.

Introduction

Recently, we have initiated a "synthetic analogue approach"[1] to metallobleomycins (M-BLM) and reported the structures and spectral properties of Cu(II) complexes of two peptides resembling portions of the metal-chelating region of the glycopeptide antibiotics, bleomycins (BLM).[2] Design of suitable yet simple organic frameworks as ligands in these complexes reduced the structural complexities encountered with BLM but retained most of the proposed donor centers around copper in Cu(II)-BLM. Such attempts allowed precise structure determination and correlation between the structure and various spectroscopic properties. Since in vivo DNA damage by BLM is attributed to an iron complex,[3] structural and spectroscopic information on the iron complexes of the synthetic organic fragments is of considerable importance. We report in this paper the synthesis, molecular structure, and spectral properties of the Fe(III) complex of one of the peptides namely, *N*-(2-(4-imidazolyl)ethyl)pyridine-2-carboxamide (**1**). Hereafter, the peptide is abbreviated at PypepH, the dissociable H being the amide H. This tailored ligand mimics three of the six proposed donor centers in Fe(III)-BLM.[3] Though Fe(III)-BLM is incapable of causing DNA strand scission, "activated

[†] University of California.
[‡] University of Windsor.

(1) Ibers, J. A.; Holm, R. H. *Science (Washington, D.C.)* **1980**, *209*, 223.
(2) Brown, S. J.; Tao, X.; Stephan, D. W.; Mascharak, P. K. *Inorg. Chem.* **1986**, *25*, 3377.
(3) Dabrowiak, J. C. *Adv. Inorg. Biochem.* **1983**, *4* and references therein.

0020-1669/87/1326-0754$01.50/0

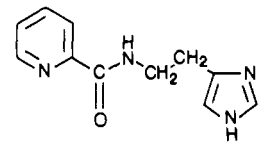

PypepH (1)

BLM" can be synthesized by reaction of H_2O_2 with Fe(III)–BLM.[4] Thus, the compound $[Fe(Pypep)_2]Cl\cdot 2H_2O$ (**2**) reported in this paper is expected to provide insight into the nature of "activated BLM". In addition to interesting solution chemistry, **2** affords structural information pertinent to Fe(III)–BLM.

Experimental Section

Preparation of Compounds. The ligand PypepH (**1**) was synthesized by the published procedure.[2] $(Et_4N)[FeCl_4]$ was prepared by mixing anhydrous $FeCl_3$ (Aldrich Chemical Co.) and Et_4NCl in ethanol. The solid thus isolated was recrystallized from acetonitrile/ethanol before use.

$[Fe(Pypep)_2]Cl\cdot 2H_2O$ (2). A solution of 327.4 mg (1 mmol) of $(Et_4N)[FeCl_4]$ in 50 mL of warm ethanol was slowly added with stirring to a solution of 864 mg (4 mmol) of PypepH in 20 mL of ethanol. The resulting deep red solution was stirred for 1 h and then stored at room temperature for 24 h. Next, the volume of the solution was reduced to ca. 15 mL under reduced pressure, and the mixture was filtered to remove a small amount of light yellow precipitate. The filtrate was then kept in a closed jar containing diethyl ether to allow slow diffusion of ether into the ethanol solution. Dark red crystals formed within 24 h. The crystals were collected by filtration after 72 h, washed with ~10 mL 1:1 v/v diethyl ether/ethanol and dried in air: yield 430 mg (77%); mp 162–165 °C (dec). Anal. Calcd for $C_{22}H_{26}N_8O_4FeCl$: C, 47.40; H, 4.67; N, 20.13; Cl, 6.37; Fe, 10.01. Found: C, 47.20; H, 4.76; N, 20.16; Cl, 6.21; Fe 9.89. Selected IR bands (KBr pellet, cm^{-1}): 3320 (s, br), 3160 (s), 2920 (m), 1595 (ν_{CO}, vs). 1395 (s), 1200 (m), 1040 (w), 840 (m), 770 (m), 690 (m), 630 (m), 500 (m).

X-ray Data Collection and Reduction. Dark red-brown crystals of **2** were obtained by slow diffusion of diethyl ether into an ethanolic solution. Diffraction experiments were performed on a four-circle Syntex $P2_1$ diffractometer with graphite-monochromatized Mo Kα radiation. The orientation matrix and lattice parameters were obtained from 15 machine-centered reflections selected from rotation photographs. These data were used to determine the crystal system. Machine parameters, crystal data, and data collection parameters are summarized in Table I. Partial rotation photographs around each axis were consistent with a triclinic crystal system ($P1$ or $P\bar{1}$ space group) Solution and refinement of the structure confirmed the space group $P\bar{1}$; the $\pm h,\pm k,+l$ data were collected in one shell ($4.5° < 2\theta < 40°$). Three standard reflections were recorded after every 197 reflections. Their intensities showed no statistically significant change over the duration of data collection. The data were processed by using the SHELX-76 program package.[5] A total of 1938 reflections with $F_o^2 > 3\sigma F_o^2$ was used in the refinement. Since the absorption coefficient was small ($\mu = 5.19$ cm^{-1}), no absorption correction was applied to the data.

Solution and Refinement of the Structure. Atomic scattering factors were taken from the literature tabulation.[6] The position of the Fe atom was determined by the heavy atom (Patterson) method. The remaining non-hydrogen atoms were located from subsequent difference Fourier maps. Refinement was carried out by using full-matrix least-squares procedure. The function minimized was $\sum w(|F_o| - |F_c|)^2$ where the weight $w = 4F_o^2/\sigma^2(F_o^2)$ and F_o and F_c are the observed and calculated structure factor amplitudes. Anisotropic temperature factors were assigned to Fe, N, O, and Cl atoms in the final stage of refinement. All carbon atoms were given isotropic thermal parameters. Hydrogen atom positions were allowed to ride on the C, O, or N atom to which they are bonded with an assumed C–H bond length of 0.95 Å and O–H and N–H bond lengths of 1.01 Å. Hydrogen atom temperature factors were fixed at 1.10 times the isotropic temperature factor of the atom to which they are bonded. In all cases, the hydrogen atom contributions were calculated but not refined. The final R factors and the maximum Δ/σ value in the final least-squares cycle are given in Table I. A final difference Fourier map showed no peak of chemical significance; the magnitude and associated atom of the largest residual electron density are included in Table I. The following data are tabulated: positional parameters (Table II); selected bond distances and angles (Table III); thermal parameters (Table S1); hydrogen atom parameters (Table S2); calculated and observed structure factors (Table S3). The last three sets of data have been deposited as supplementary material.

Table I. Crystallographic Parameters for $[Fe(Pypep)_2]Cl\cdot 2H_2O$ (**2**)

formula (M_r)	$C_{22}H_{26}ClFeN_8O_4$ (557.3)
cryst color, form	red-brown block
a, Å	11.080 (5)
b, Å	9.319 (4)
c, Å	13.665 (5)
α, deg	112.75 (3)
β, deg	103.92 (3)
γ, deg	73.53 (3)
cryst syst	triclinic
V, Å^3	1234.1 (9)
Z	2
d_{calcd}, g/cm^3	1.50
d_{obsd},[a] g/cm^3	1.49
space group	$P\bar{1}$
cryst dimens, mm	0.38 × 0.29 × 0.35
radiation	Mo Kα (λ = 0.71069 Å)
abs coeff (μ), cm^{-1}	5.19
temp, °C	24
scan speed, deg/min	2.0–5.0 ($\theta/2\theta$ scan)
scan range, deg	1.0 below Kα_1 to 1.0 above Kα_2
bkgd/scan time ratio	0.5
no. of data collcd	2439
no. of unique data ($F_o^2 > 3\sigma(F_o^2)$)	1938
no. of variables	215
R,[b] %	4.46
R_w,[c] %	5.39
largest Δ/σ in the final least-squares cycle	0.001
max residual electron density, e/Å^3	0.50 (assoc with C9)

[a] Determined by flotation in CCl_4/cyclohexane. [b] $R = \sum||F_o| - |F_c||/\sum|F_o|$. [c] $R_w = [\sum w(|F_o| - |F_c|)^2/\sum w|F_o^2|)]^{1/2}$.

Other Physical Measurements. Absorption spectra were obtained with either a Cary Model 14 or Hitachi Model 100-80 spectrophotometer. Infrared spectra were measured on a Nicolet MX-S FTIR spectrometer. Electrochemical measurements were performed with standard Princeton Applied Research instrumentation using a Pt or a glassy-carbon working electrode; potentials were measured at ~25 °C vs. a saturated calomel electrode as reference. ^1H NMR spectra were recorded on a General Electric 300-MHz GN-300 instrument in CD_3OD (99.9% D). Chemical shifts downfield and upfield of the Me_4Si reference are designated as negative and positive, respectively. Solution magnetic susceptibility was determined by the conventional NMR method in Me_4Si solution,[7] and reference shift differences were measured to ±0.2 Hz by using 30–40 mM solutions of **2** in CD_3OD in coaxial tubes. Solvent susceptibility[8] and diamagnetic corrections[9] were taken from published data. Mössbauer spectra were obtained with a constant-acceleration spectrometer in the temperature range 4.2–298 K. Polycrystalline samples were dispersed in boron nitride powder. Spectra were measured in a zero applied magnetic field and all ^{57}Fe isomer shifts are quoted vs. Fe metal at room temperature. EPR spectra were recorded on a Varian E-3 spectrometer connected to a Digital PDP-11 computer for data manipulation. Samples were run at 9 GHz (X-band) in the temperature range 77–298 K. Elemental analyses were performed by Atlantic Microlab Inc., Atlanta, GA. The % Fe was determined by EDTA titration with variamine blue used as the indicator.[10]

Results and Discussion

The complex bis(N-(2-(4-imidazolyl)ethyl)pyridine-2-carboxamido)iron(III) chloride dihydrate (**2**) belongs to a moderately small group of iron complexes containing low-spin iron(III) in a non-heme octahedral N_6 chromophore. The other known ex-

(4) Kuramochi, H.; Takahashi, K.; Takita, T.; Umezawa, H. *J. Antibiot.* **1981**, *34*, 576. Burger, R. M.; Peisach, J.; Horwitz, S. B. *J. Biol. Chem.* **1981**, *256*, 11636.
(5) Sheldrick, G. M. *SHELX-76, Program for Crystal Structure Determination*; University of Cambridge: Cambridge, England, 1976.
(6) Cromer, D. T.; Waber, J. T. *International Tables for X-ray Crystallography*; Kynoch: Birmingham, England, 1974; Vol. IV. Stewart, R. F.; Davidson, E. R.; Simpson, W. T. *J. Chem. Phys.* **1965**, *42*, 3175.
(7) Evans, D. F. *J. Chem. Soc.* **1959**, 2003. Phillips, W. D.; Poe, M. *Methods Enzymol.* **1972**, *24*, 304.
(8) Gerger, W.; Mayer, V.; Gutmann, V. *Monatsch. Chem.* **1977**, 417.
(9) Mulay, L. N. In *Physical Methods of Chemistry*; Weissberger, A., Rossiter, B. W., Eds.; Wiley-Interscience: New York, 1972; Part IV, Chapter VII.
(10) Vogel, A. In *Textbook of Quantitative Inorganic Analysis*; Longman: New York, 1978; p 322.

Table II. Positional Parameters ($\times 10^4$) for $[Fe(Pypep)_2]Cl\cdot 2H_2O$ (**2**)

atom	x	y	z	atom	x	y	z
Fe	7348 (1)	7660 (1)	7508 (1)	O1	5133 (4)	6671 (5)	4630 (3)
O2	10846 (3)	8628 (5)	8713 (3)	O3	4652 (4)	2310 (5)	6997 (3)
O4	12902 (4)	6032 (5)	8354 (4)	N1	6448 (4)	9498 (5)	8561 (3)
N2	6010 (4)	11817 (5)	9826 (3)	N3	5793 (4)	7550 (5)	6459 (3)
N4	8050 (4)	5870 (5)	6282 (3)	N5	7041 (4)	6179 (5)	8066 (3)
N6	6300 (4)	4334 (5)	8214 (4)	N7	8992 (4)	7768 (5)	8436 (3)
N8	7900 (4)	9112 (5)	7042 (3)	C1	5138 (5)	9962 (6)	8550 (4)
C2	4870 (6)	11400 (7)	9328 (4)	C3	6921 (5)	10663 (6)	9357 (4)
C4	4262 (5)	8962 (7)	7748 (4)	C5	4501 (5)	8489 (6)	6612 (4)
C6	5951 (5)	6697 (6)	5448 (5)	C7	7227 (5)	5655 (6)	5352 (4)
C8	7567 (6)	4534 (7)	4400 (5)	C9	8742 (6)	3525 (8)	4410 (5)
C10	9559 (6)	3683 (7)	5344 (5)	C11	9195 (5)	4894 (6)	6284 (4)
C12	6275 (5)	5138 (6)	7593 (4)	C13	7124 (5)	4860 (7)	9130 (5)
C14	7591 (5)	6002 (6)	9051 (4)	C15	8514 (5)	6973 (7)	9804 (4)
C16	9538 (5)	7004 (7)	9254 (5)	C17	9718 (5)	8540 (6)	8289 (4)
C18	9073 (5)	9393 (6)	7527 (4)	C19	9604 (6)	10407 (7)	7335 (5)
C20	8920 (6)	11178 (8)	6623 (5)	C21	7731 (6)	10887 (7)	6110 (5)
C22	7248 (5)	9854 (6)	6352 (4)	Cl	1918 (2)	12864 (2)	7529 (2)

Table III. Selected Bond Distances and Angles for $[Fe(Pypep)_2]Cl\cdot 2H_2O$ (**2**)

		Distances (Å)			
Fe–N1	1.953 (4)	Fe–N3	1.957 (4)	Fe–N4	1.981 (4)
Fe–N5	1.951 (4)	Fe–N7	1.958 (4)	Fe–N8	1.983 (4)
N1–C1	1.389 (6)	N1–C3	1.331 (7)	C1–C2	1.356 (7)
C1–C4	1.491 (7)	C2–N2	1.368 (7)	N2–C3	1.322 (7)
C4–C5	1.508 (7)	C5–N3	1.467 (7)	N3–C6	1.327 (7)
C6–O1	1.255 (6)	C6–C7	1.474 (8)	C7–N4	1.355 (7)
C7–C8	1.374 (7)	C8–C9	1.374 (8)	C9–C10	1.357 (8)
C10–C11	1.399 (8)	C11–N4	1.335 (7)	N5–C12	1.341 (7)
N5–C14	1.389 (6)	C12–N6	1.323 (7)	N6–C13	1.368 (7)
C13–C14	1.357 (7)	C14–C15	1.491 (7)	C15–C16	1.515 (8)
C16–N7	1.473 (7)	N7–C17	1.312 (7)	C17–O2	1.256 (6)
C17–C18	1.478 (7)	C18–N8	1.357 (7)	C18–C19	1.375 (8)
C19–C20	1.384 (8)	C20–C21	1.389 (9)	C21–C22	1.396 (8)
C22–N8	1.334 (7)				
		Angles (deg)			
N1–Fe–N3	91.0 (2)	N1–Fe–N4	171.6 (2)	N1–Fe–N5	92.1 (2)
N1–Fe–N7	92.8 (2)	N1–Fe–N8	89.9 (2)	N3–Fe–N4	81.0 (2)
N3–Fe–N5	93.3 (2)	N3–Fe–N7	173.8 (2)	N3–Fe–N8	94.3 (2)
N4–Fe–N5	91.0 (2)	N4–Fe–N7	94.9 (2)	N4–Fe–N8	88.2 (2)
N5–Fe–N7	91.4 (2)	N5–Fe–N8	172.2 (2)	N7–Fe–N8	80.9 (2)
Fe–N1–C1	126.3 (3)	Fe–N1–C3	128.1 (4)	C1–N1–C3	105.2 (4)
N1–C1–C2	108.8 (4)	N1–C1–C4	121.3 (4)	C1–C2–N2	106.6 (5)
C2–N2–C3	107.8 (4)	N2–C3–N1	111.6 (5)	C1–C4–C5	112.7 (4)
C4–C5–N3	112.1 (4)	C5–N3–Fe	128.2 (3)	C5–N3–C6	115.0 (4)
N3–C6–O1	126.8 (5)	N3–C6–C7	112.5 (5)	C6–C7–C8	123.2 (5)
C6–C7–N4	114.9 (4)	C8–C7–N4	121.9 (4)	C7–C8–C9	118.7 (6)
C8–C9–C10	120.0 (4)	C9–C10–C11	119.3 (6)	C10–C11–N4	121.1 (5)
C7–N4–C11	118.9 (4)	C11–N4–Fe	127.8 (4)	C7–N4–Fe	113.3 (3)
Fe–N5–C12	127.8 (4)	Fe–N5–C14	125.9 (3)	C12–N5–C14	106.2 (4)
N5–C12–N6	111.0 (5)	C12–N6–C13	107.3 (5)	N6–C13–C14	108.1 (5)
C13–C14–N5	107.3 (5)	C13–C14–C15	131.3 (5)	N5–C14–C15	121.4 (5)
C14–C15–C16	112.6 (5)	C15–C16–N7	111.3 (5)	C16–N7–C17	115.9 (4)
C16–N7–Fe	126.9 (3)	Fe–N7–C17	117.2 (3)	N7–C17–O2	128.0 (5)
N7–C17–C18	113.1 (5)	C17–C18–C19	123.1 (5)	C17–C18–N8	114.5 (5)
C19–C18–N8	122.4 (5)	C18–C19–C20	119.1 (6)	C19–C20–C21	119.1 (6)
C20–C21–C22	118.6 (6)	C21–C22–N8	122.5 (5)	C22–N8–Fe	127.9 (4)
C22–N8–C18	118.2 (5)				

amples include $[Fe^{III}L_3]^{n+}$ complexes with L = ethylenediamine (en),[11] 1,10-phenanthroline (phen),[12-14] 2,2′-bipyridyl (bpy),[12,13,15] 2-(2-pyridyl)imidazole(pyimH),[16] and $[Fe^{III}L_2]^{n+}$ complexes with L = 2,2′,2″-terpyridine (terpy),[17] 1,4,7-triazacyclononane (tacn),[18] and hydrotripyrazolylborate ($HB(pz)_3$).[19] There is a recent report on a mononuclear iron(III) complex with a hexadentate, potentially binucleating, bimacrocyclic ligand 1,2-bis(1,4,7-triaza-1-cyclononyl)ethane (dtne).[20] The phen, bpy, and terpy complexes are conveniently obtained by oxidation of the corresponding iron(II) complexes with PbO_2 in ~1 M H_2SO_4 followed by addition of a suitable noncoordinating anion like ClO_4^- or PF_6^-.[13]

(11) Renovitch, G. A.; Baker, W. A., Jr. *J. Am. Chem. Soc.* **1968**, *90*, 3585.
(12) Schilt, A. A. *J. Am. Chem. Soc.* **1960**, *82*, 3000. Figgis, B. N. *Trans. Faraday Soc.* **1961**, *57*, 204.
(13) DeSimone, R. E.; Drago, R. S. *J. Am. Chem. Soc.* **1970**, *92*, 2343.
(14) Baker, J.; Engelhardt, L. M.; Figgis, B. N.; White, A. H. *J. Chem. Soc., Dalton Trans.* **1975**, 530.
(15) Figgis, B. N.; Skelton, W.; White, A. H. *Aust. J. Chem.* **1978**, *31*, 57.
(16) Chiswell, B.; Lions, F.; Morris, B. S. *Inorg. Chem.* **1964**, *3*, 110.
(17) Reiff, W. M.; Baker, W. A., Jr.; Erickson, N. E. *J. Am. Chem. Soc.* **1968**, *90*, 4794.
(18) Wieghardt, K.; Schmidt, W.; Herrmann, W.; Küppers, H.-J. *Inorg. Chem.* **1983**, *22*, 2953. Boeyens, J. C. A.; Forbes, A. G. S.; Hancock, R. D.; Wieghardt, K. *Inorg. Chem.* **1985**, *24*, 2926.
(19) Armstrong, W. H.; Spool, A.; Papaefthymiou, G. C.; Frankel, R. B.; Lippard, S. J. *J. Am. Chem. Soc.* **1984**, *106*, 3653.
(20) Wieghardt, K.; Tolksdorf, I.; Herrmann, W. *Inorg. Chem.* **1985**, *24*, 1230.

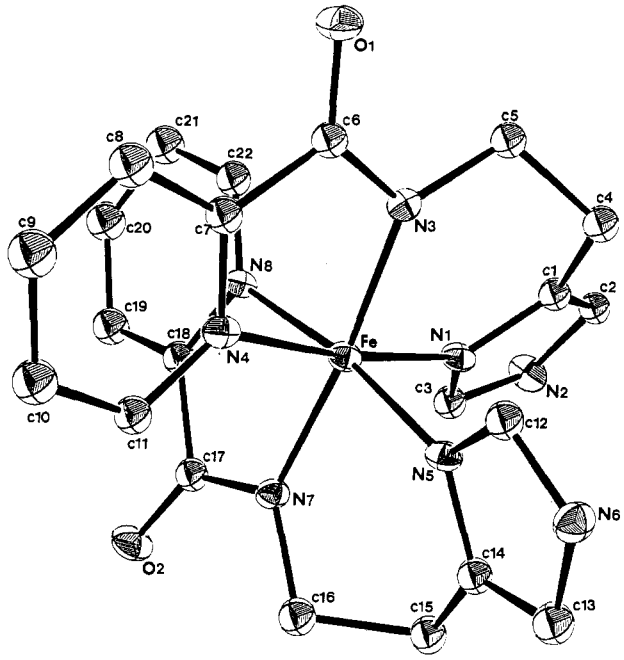

Figure 1. Structure of $[Fe(Pypep)_2]^+$ (**2**), showing 50% probability ellipsoids and the atom-labeling scheme. Hydrogen atoms have been omitted for clarity.

Direct addition of terpy to iron(III) salts results in rapid reduction and formation of $[Fe(terpy)_2]^{2+}$.[17] However, with **1**, no reduction is evident (vide infra), and **2** is isolated in high yield from the reaction mixture containing $(Et_4N)[FeCl_4]$ and excess (4 equiv) PypepH in ethanol. The water molecules present in the crystalline product are most probably derived from the atmosphere during the long crystallization step.

Structure of $[Fe(Pypep)_2]Cl\cdot 2H_2O$ (2). An ORTEP drawing of the cation is shown in Figure 1. The coordination geometry around the iron atom is octahedral. The three nitrogens of the peptide ligand **1** are bonded to the iron atom with the pyridine and the imidazole N atoms being trans to one another. The two deprotonated peptide N atoms of the two ligands are trans to each other. Thus the tridentate anionic ligand gives rise to a *mer* isomer. In this regard, **1** resembles terpy.[17] In contrast, the three N donors in tacn,[18] 1,2,3-triaminopropane (ptn),[21] and hydrotripyrazolylborate $(HBpz_3)$[19] can only coordinate facially.

Selected bond distances and angles for **2** are listed in Table III. The Fe(III)–N_{py} (py = pyridine) distance of 1.982 (4) Å is very close to the mean Fe(III)–N distance of 1.973 Å in $[Fe(phen)_3](ClO_4)_3\cdot H_2O$.[16] The average Fe(III)–N_{py} distance in $(bpyH)[Fe(bpy)_3](ClO_4)_4$ is slightly shorter (1.963 Å).[15] In the low-spin ferric tetraphenylporphyrin (TPP) complexes $[Fe(TPP)(N_3)(py)]$[22] and $[Fe(TPP)(NCS)(py)]$,[23] where the iron atom is essentially coplanar with the porphinato nitrogen atoms, the Fe(III)–N_{py} bond lengths are 2.089 (6) and 2.082 (3) Å, respectively. This lengthening has been attributed to steric interactions between the porphinato core and the pyridine ring. The Fe(III)–N_{im} (im = imidazole) bonds in **2** are 1.952 (4) Å long. Hoard and co-workers[24] have estimated that the Fe(III)–N_{im} bond length in the unconstrained $[Fe(TPP)(im)_2]^+$ cation would be close to 1.95 Å. It is, therefore, evident that the Fe(III)–N_{im} bond length is close to 1.95 Å in both heme (unconstrained) and non-heme low-spin Fe(III) complexes containing N_6 chromophore. The Fe–N_{pz} (pz = pyrazole) distance (1.957 Å) in low-spin $[Fe(HB(pz)_3)_2]^+$ is also very close to this value.[19]

It has been stated that in general Fe(III) has no propensity of promoting amide deprotonation with concomitant coordination of the negative amido nitrogen donor centers.[25] However, Martell and co-workers have reported stable Fe(III) chelates of multidentate ligands containing amide linkages.[26] The ability of these ligands to coordinate to Fe(III) via amide deprotonation has been ascribed in part to the presence of additional coordinating donor groups that serve to prevent hydrolysis and separation of ferric hydroxide. Unfortunately no structural data on these complexes are available. The successful isolation and structure determination of **2** thus support Martell's suggestion and provide a value of 1.985 (4) Å for the Fe(III)–N(amido) bond.

The N–Fe–N angles that show maximum deviation from octahedral values are the angles N3–Fe–N4 (81.0 (2)°) and N7–Fe–N8 (80.9 (2)°). This might arise from the presence of a short (bond order >1) amide C–N bond in the five-membered chelate rings. Further evidence of strain in the five-membered chelate rings comes from the C6–C7–N4 (114.9 (4)°) and C17–C18–N8 (114.5 (5)°) angles, which depart from the normal sp^2 angle of 120°. The bond distances and angles in the six-membered chelate rings are however, normal. The trans N atoms around iron are drawn to each other to some extent such that the N–Fe–N angles are all close to 172° (Table III). The geometries of the pyridine and imidazole rings are rather regular.

The chloride ion is hydrogen bonded to the two water molecules (W1 and W2) and is located halfway between them ($Cl\cdots H_a(W1)$ = 2.139 Å, $Cl\cdots H_a(W2)$ = 2.142 Å). The other hydrogen atoms (H_b) of W1 and W2 are hydrogen bonded to peptide O atoms of two neighboring cations ($H_b\cdots O2$(cation 1) = 1.878 Å, $H_b\cdots O2$(cation 2) = 1.824 Å). Thus the two water molecules and the chloride ion bridge two cations through hydrogen bonding.

Properties. The low-spin configuration of Fe(III) in **2** has been confirmed by its variable-temperature Mössbauer spectra in

Table IV. Spectroscopic and Electrochemical Data for $[Fe(Pypep)_2]Cl\cdot 2H_2O$ (**2**)

Mössbauer Spectrum[a]

T, K	δ,[b,c] mm/s	ΔE_Q,[c] mm/s
298	0.10	1.28
160	0.16	1.49
80	0.18	1.57
4.2	0.18	1.59

^1H Chemical Shifts (ppm; ~298 K, CD_3OD Solution)

−120.80, −15.45, −11.14, −9.26, −7.38, −5.06, −3.39, −1.24, 4.81, 27.71

Half-Wave Potential[d]

solvent	$E_{1/2}$,[e] V (ΔE_p[f])	solvent	$E_{1/2}$,[e] V (ΔE_p[f])
H_2O	−0.28 (60)	DMF	−0.31 (70)
MeOH	−0.17 (90)	Me_2SO	−0.33 (80)
MeCN	−0.33 (70)		

Electronic Spectrum

solvent	λ_{max}, nm (ϵ, M^{-1} cm^{-1})
H_2O[g]	500 sh (1100), 450 (1400), 385 sh (3700), 360 (4300), 255 (12200)
MeOH	505 (1570), 450 sh (1400), 380 sh (3700), 365 (4100), 255 (12000)
Me_2SO	515 (2100), 450 sh (1400), 390 sh (3800), 370 (4300)

[a] In boron nitride matrix. [b] Relative to Fe metal at room temperature. [c] Estimated uncertainties are ±0.03 mm/s in δ and ±0.05 mm/s in ΔE_Q. [d] Cyclic voltammetry, Beckman Pt-inlay electrode, 0.1 M tetrabutylammonium perchlorate as supporting electrolyte except for the aqueous solution, which was 0.1 M in KCl, 50 mV/s scan speed. [e] Values quoted vs. aqueous SCE. [f] Peak to peak separation in mV. [g] pH 7.4.

(21) Henrick, K.; McPartlin, M.; Munjoma, S.; Owston, P. G.; Peters, R.; Sangokoya, S. A.; Tasker, P. A. *J. Chem. Soc., Dalton Trans.* **1982**, 225.
(22) Adams, K. M.; Rasmussen, P. G.; Scheidt, W. R.; Hatano, K. *Inorg. Chem.* **1979**, *18*, 1892.
(23) Scheidt, W. R.; Lee, Y. J.; Geiger, D. K.; Taylor, K.; Hatano, K. *J. Am. Chem. Soc.* **1982**, *104*, 3367.
(24) Collins, D. M.; Countryman, R.; Hoard, J. L. *J. Am. Chem. Soc.* **1972**, *94*, 2066.
(25) Sigel, H.; Martin, R. B. *Chem. Rev.* **1982**, *82*, 385.
(26) Motekaitis, R. J.; Martell, A. E. *J. Am. Chem. Soc.* **1970**, *92*, 4223; **1982**, *104*, 3782. Smith, R. M.; Motekaitis, R. J.; Martell, A. E. *Inorg. Chem.* **1985**, *24*, 1132.

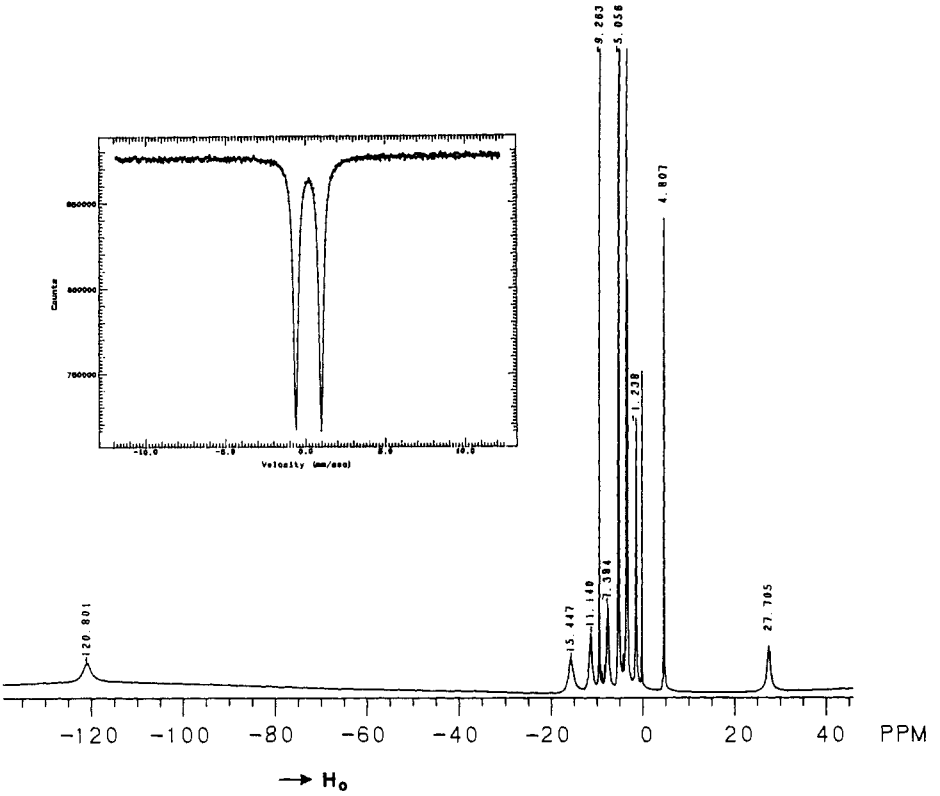

Figure 2. ^{1}H NMR spectrum (300 MHz, ~298 K) of $[Fe(Pypep)_2]Cl\cdot 2H_2O$ (**2**) in CD_3OD. Insert: Zero-field Mössbauer spectrum of polycrystalline **2** at 4.2 K. The solid line is a theoretical least-squares fit to the data assuming Lorentzian line shapes.

polycrystalline state and magnetic susceptibility measurement in CD_3OD solution at room temperature. The Mössbauer spectral parameters for **2** in the temperature range 4.2–298 K obtained by computer fitting of the experimental spectra with Lorentzian line shapes are collected in Table IV, and the spectrum recorded at 4.2 K is shown in Figure 2. The small isomer shifts (δ) observed at various temperatures indicate a low-spin iron complex and result from an increased involvement of the iron 4s orbital in covalent bonding with ligands with strong π-acceptor properties.[27] Since isomer shifts for low-spin octahedral ferrous (t_{2g}^6) and ferric (t_{2g}^5) complexes are rather similar, δ is not a good diagnostic of the oxidation state, unlike the case of the high-spin complexes. However, it is important to note that the value of the quadrupole splitting (ΔE_Q) for **2** is temperature dependent (Table IV).[28] With low-spin Fe(III), the thermal population of the "electron-hole" in the t_{2g} orbital manifold in a distorted octahedral crystal field results in a temperature dependence of the quadrupole splitting parameter that is not observed with low-spin Fe(II) complexes.[29] Thus, the isomer shift values combined with the temperature dependence of the quadrupole splitting parameter confirm the presence of low-spin Fe(III) in **2**. The quadrupole splittings (80 K) of $[Fe(en)_3]Cl_3$ (1.09 mm/s), $[Fe(phen)_3](ClO_4)_3\cdot H_2O$ (1.71 mm/s), $[Fe(bpy)_3](ClO_4)_3$ (1.80 mm/s), and $[Fe(terpy)_3](ClO_4)_3$ (3.43 mm/s) show that the degree of distortion from octahedral symmetry increases in the order en < phen < bpy < terpy.[30] It is, therefore, evident from Table IV that the peptide ligand **1** can be placed in between en and phen in the sequence. This indicates that the symmetry of the crystal field around iron in **2** is close to regular octahedral and is consistent with the crystallographic data.

At ambient temperature, the effective magnetic moment of low-spin Fe(III) lies in the range 2.0–2.6 μ_B.[31] The doublet ground state gives rise to higher magnetic moment (>1.73 μ_B) due to orbital contribution.[32] In the present case, magnetic susceptibility measurement in CD_3OD solution at 298 K yields an effective magnetic moment of 2.24 μ_B, which also supports the low-spin ($S = {}^1/_2$) configuration of Fe(III) in **2**.

At liquid N_2 temperature, **2** is essentially EPR silent both in polycrystalline state and in methanol glass—only a very weak g = 4.3 transition due to paramagnetic high-spin iron impurity is observed. With octahedral low-spin d^5 ($S = {}^1/_2$) systems, EPR spectra can be seen only at very low temperature (~4 K) because of strong spin–orbit coupling interaction.[33] Large deviations from octahedral symmetry can cause an orbitally singlet state to lie very low in energy, giving rise to long electron relaxation times, and EPR spectra can be observed at higher temperature. Though the low-spin d^5 system is subject to Jahn–Teller distortion, the structure of $[Fe(Pypep)_2]^+$ is quite regular. Thus no EPR spectrum is observed with **2** at 80 K. EPR spectra of the phen and bpy complexes have been obtained at 77 K either with single crystals or with samples doped into suitable diamagnetic host lattice.[13-15] Similar measurements with **2** are in progress and the results will be reported elsewhere.

The 300-MHz ^{1}H NMR spectrum of **2** in CD_3OD is shown in Figure 2. Several paramagnetically shifted resonances are observed (Table IV). The two molecules of water present in the crystalline sample of **2** exhibit a resonance at −5.06 ppm. Recently, Sugiura et al. have reported the NMR spectra of Fe(III)–BLM–N_3 and Fe(III)–BLM–CH_3NH_2 adducts.[34] These complexes contain low-spin ferric iron in an FeN_6 chromophore.[35] Contrary to Figure 2, Sugiura et al. could record only one peak for each of the compounds at −17.2 and −25.1 ppm (vs. TSP), respectively. The small paramagnetic shifts have been ascribed to low-spin ferric

(27) Greenwood, N. N.; Gibb, T. C. In *Mössbauer Spectroscopy*; Chapman and Hall: London, 1971; Chapter VII, p 169.
(28) The small temperature dependence of the isomer shift in Table IV is due to the second-order Doppler shift.
(29) Merrithew, P. B.; Lo, C.-C.; Modestino, A. J. *Inorg. Chem.* **1973**, *8*, 1927.
(30) Reference 27, p 187.
(31) Cotton, S. A. *Coord. Chem. Rev.* **1972**, *8*, 185.
(32) Earnshaw, A. In *Introduction to Magnetochemistry*; Academic: London, 1968; p 35.
(33) Drago, R. S. In *Physical Methods in Chemistry*; Saunders: Philadelphia, 1977; Chapter XIII, pp 492–493.
(34) Sugiura, Y.; Suzuki, T.; Kawabe, H.; Tanaka, H.; Watanabe, K. *Biochim. Biophys. Acta* **1982**, *716*, 38.
(35) Sugiura, Y. *J. Am. Chem. Soc.* **1980**, *102*, 5208.

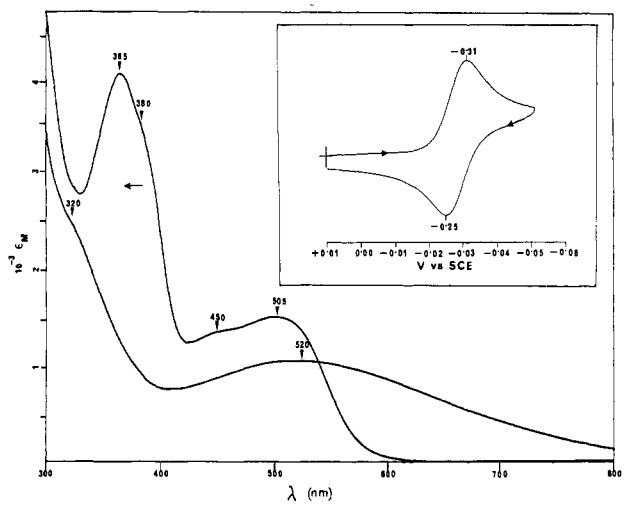

Figure 3. Absorption spectrum of $[Fe(Pypep)_2]Cl\cdot 2H_2O$ (**2**) (upper curve) and the reduced species derived from **2** upon reduction with L-ascorbic acid (lower curve) in methanol solution. Insert: Cyclic voltammogram (50 mV/s) of **2** at a Pt electrode in aqueous (0.1 M KCl) solution.

($S = {}^1/_2$) state. Since a magnetic susceptibility measurement on the NMR sample at the same temperature confirms the $S = {}^1/_2$ state for Fe(III) in **2**, we believe that not all resonances for the Fe(III)–BLM adducts have been located. With **2**, peaks at −120.80 and +27.71 ppm do not disappear on D_2O exchange. Instead, chemical shifts for both the peaks change to more positive values with an increasing amount of D_2O in solution. At the present time, work is in progress to assign the various resonances in the NMR spectrum of **2**.

In protic and aprotic media, **2** exhibits a clean one electron-redox process. The cyclic voltammogram of **2** in water is shown in Figure 3, and the half-wave potential ($E_{1/2}$) values in different solvents are collected in Table IV. The redox process is reversible ($i_c/i_a = 1$, $\Delta E_p = 60$ mV) in water[36] and approaches reversibility in the other solvents used. Voltammetric characteristics are practically identical on both glassy-carbon and Pt electrodes. Electrochemical studies on several low-spin Fe(III) complexes containing FeN_6 chromophore have been reported.[37] The $E_{1/2}$ values for $[Fe(phen)_3]^{3+/2+}$ and $[Fe(bpy)_3]^{3+/2+}$ couples in aqueous solution (pH ≈2) are +0.89 and +0.87 V (vs. SCE), respectively.[28] These $E_{1/2}$ values indicate that the aromatic heterocyclic ligands stabilize the +2 oxidation state. Such stabilization is not provided by the aliphatic polyamine ligands. The most negative $E_{1/2}$ value recorded for a low-spin FeN_6 chromophore is associated with $[Fe(tacn)_2]^{3+}$, which in aqueous KCl solution (0.1 M) exhibits a reversible redox process at −0.11 V vs. SCE.[18] With **2**, the $E_{1/2}$ value is even more negative (−0.28 V vs. SCE). Thus, the peptide ligand **1** appears to provide the maximum stabilization to Fe(III) among all the reported low-spin Fe(III) complexes with N-only donors. Also with **2**, the +3 oxidation state is found to be more stable in aprotic solvents like DMF and Me_2SO, while protic solvents stabilize the Fe(II) species (Table IV). The same trend is observed with the phen and bpy complexes.[39]

Though the reduced form of **2** is stable on voltammetric time scale, it undergoes slow chemical decomposition in solution. On exhaustive electrolysis at −0.40 V (vs. SCE) in methanol, the dark red solution of **2** first turns to deep purple, which then slowly fades in color with precipitation of an off-white solid. Similar behavior is also noted when attempts are made to record the absorption spectrum of the reduced species generated chemically (vide infra). The rate of decomposition is, however, decelerated in the absence of oxygen. The reduced species in the purple solution exhibits a few ill-defined voltammetric responses along with the one associated with $[Fe(Pypep)_2]^{3+/2+}$ couple.

The UV-visible spectrum of **2** in methanol is displayed in Figure 3, and absorption parameters in different solvents are listed in Table IV. The dark red color of **2** results from a strong absorption ($\epsilon \sim 1500$ M^{-1} cm^{-1}) in the region 400–500 nm. There is a second and more intense ($\epsilon \sim 4000$ M^{-1} cm^{-1}) absorption at ~360 nm. Although we do not have enough information to assign completely the electronic spectrum of **2**, a couple of comments can be made. Both the ~450- and ~360-nm absorptions arise from ligand-to-metal charge transfer (LMCT) since they are either weak or absent in the spectrum of the reduced species (Figure 3). Also, intense ($\epsilon \sim 5000$ M^{-1} cm^{-1}) absorption at 440 nm is noted with the dark red solution of $[Fe(HBpz_3)_2]^+$ in acetonitrile but not with orange-red $[Fe(tacn)_2]^{3+}$.[40] With the latter complex, the absorptions are most possibly due to d–d transitions of the low-spin d^5 system, which, in the case of **2**, are hidden under the intense LMCT bands.

When one equivalent of L-ascorbic acid is added to a solution of **2** in methanol or water, the color changes from red to purple. The absorption spectrum of the purple solution, presumably containing the reduced species, in methanol is shown in Figure 3. The purple solution is air-sensitive and is decomposed readily with precipitation of an off-white solid. Reduction can also be achieved with dithiothreitol. However, in such attempts, the purple solution decomposes with precipitation of a brown solid even in the absence of oxygen. The orange-yellow solution of Fe(III)–BLM undergoes facile reduction with sodium dithionite and L-ascorbic acid.[35] The pale pink solution containing Fe(II)–BLM has a visible absorption maximum at 475 nm ($\epsilon = 380$) and is air-sensitive. We believe that once isolated, the reduced species from **2** will help in elucidating the structure and chemistry of Fe(II)–BLM and related products. Preliminary experiments have shown that when $FeCl_2\cdot 2H_2O$ is allowed to react with 2.5 equiv of **1** in methanol under dinitrogen, a dark purple solution results and the solution exhibits an absorption spectrum identical with the one displayed in Figure 3. At the present time, attempts are being made to isolate crystalline product(s) from such solutions.

Summary

The following points are the principal results and conclusions of this investigation.

(1) The Fe(III) complex $[Fe(Pypep)_2]Cl\cdot 2H_2O$ (**2**) of the peptide ligand PypepH (**1**) has been isolated and structurally characterized. Various spectroscopic properties have established the presence of low-spin Fe(III) in an FeN_6 chromophore.

(2) The structure of **2** provides information pertinent to low-spin Fe(III)–BLM, e.g., the Fe(III)–N_{im} distance and in particular the Fe(III)–N(peptide) bond length, which is scarce in the literature.

(3) The Fe(III) complex **2** has been reduced electrochemically and chemically to Fe(II) species whose absorption spectrum has been recorded. Structural and reactivity features of the reduced species are under investigation.

Acknowledgment. This research was supported by a Faculty Research Committee Grant at the University of California, Santa Cruz and by the NSERC of Canada at the University of Windsor, Windsor, Ontario, Canada. We are also thankful to Drs. G. Papaefthymiou and R. Frankel of Francis Bitter National Magnet Laboratory, Massachusetts Institute of Technology, Cambridge, MA, for help in acquiring the Mössbauer spectra.

Supplementary Material Available: Crystal structure data for $[Fe(Pypep)_2]Cl\cdot 2H_2O$ including thermal parameters of the cation and the anion (Table S1) and hydrogen atom parameters (Table S2) (2 pages); observed and calculated structure factors (Table S3) (8 pages). Ordering information is given on any current masthead page.

(36) Nicholson, R. S.; Shain, I. *Anal. Chem.* **1964**, *36*, 706. Nicholson, R. S. *Anal. Chem.* **1965**, *37*, 1351.
(37) Heusler, K. E. In *Encyclopedia of Electrochemistry of the Elements*; Bard, A. J., Ed.; Marcel Dekker: New York, 1982; Vol. IX, Part A, pp 229–381.
(38) George, P.; Hanania, G. I. H.; Irvine, D. H. *J. Chem. Soc.* **1959**, 2548.
(39) For example, $E_{1/2}$ of values the $[Fe(phen)_3]^{3+/2+}$ couple are +0.89 and +0.70 V vs. SCE in water and acetonitrile, respectively.
(40) UV–visible absorption spectrum of $[Fe(tacn)_2]^{3+}$ (λ_{max}, nm (ϵ, M^{-1} cm^{-1})): 500 (sh), 430 (82), 336 (288).[18]